Application of the arbitrary lagrangian eulerian formulation to the numerical simulation of stationary forming processes with dominant tangential material motion

Sabine Philippe, Lionel Fourment, Pierre Montmitonnet

APPLICATION OF THE ARBITRARY LAGRANGIAN EULERIAN FORMULATION TO THE NUMERICAL SIMULATION OF STATIONARY FORMING PROCESSES WITH DOMINANT TANGENTIAL MATERIAL MOTION

Sabine PHILIPPE, Lionel FOURMENT, Pierre MONTMITONNET

CEMEF, Ecole des Mines de Paris, BP 207, 06 904 Sophia Antipolis Cedex, France

ABSTRACT

In this paper, an Arbitrary Lagrangian Eulerian (ALE) formulation has been developed for 3D FEM simulations of quasi-stationary metal forming processes (such as drawing, rolling, extrusion…). In such a formulation, the mesh is updated independently from the material motion, allowing the mesh to be continuously optimized. It is however difficult in 3D to relocate mesh nodes such that the movement of the material domain boundaries can be followed. In general, it is achieved by setting the normal component of the mesh velocity equal to the normal component of the material velocity for each boundary node. This initial choice was found unsatisfactory for processes with dominant tangential velocity. For such cases, a new procedure has been implemented in the FORGE3® software [1]. The surface nodes are projected onto the intermediate surface computed at the end of the Lagrangian virtual updating stage. Different strategies are developed to project the nodes, according to the topological entities they belong to (vertices, edges, plane or curved surfaces). A comparison for wire and bar drawing processes is provided between a standard Updated Lagrangian formulation [1] and the present ALE formulation, showing very similar results (geometry shape, drawing stress, strain rates …).

1. INTRODUCTION

The paper describes an ALE formulation, and particularly a mesh motion technique, developed in the context of stationary forming processes with dominant tangential velocity.

Different formulations, Lagrangian or Eulerian, can be used for FEM simulation of metal forming processes. In an Updated Lagrangian (UL) formulation, the mesh velocity is set equal to the material velocity. Therefore by construction, the mesh movement follows the free surfaces. A drawback of UL is the absolute need for frequent remeshing to (i) remedy severe mesh distorsion, (ii) maintain mesh refinement in critical strain and stress areas [1]. Remeshing may be CPU-time consuming and involves frequent more or less diffusive variable remapping, resulting in precision loss [2]. Another characteristics of UL which becomes a drawback when dealing with stationary processes is that modelling of the process transients is necessary. In Eulerian approaches, the mesh is fixed in space and the material flows through it [3]. It seems attractive for stationary processes: mesh quality and local, preset refinements are preserved, supposedly providing more accurate results. Obtaining an accurate description of the free surface is however a critical issue in the Eulerian formulation.

The ALE method tries to combine the advantages of both formulations. The mesh can be updated independently from the material motion. In this way, grid distortion can be avoided, mesh adaptation can be introduced and free surfaces correctly described. The steady state of a process can be directly computed, as well as the transient phases if needed. The ALE formula-

tion is so regarded as the most appropriate formulation for FEM simulations of stationary processes [4].
The ALE formulation developed in this paper is presented in Section 2. It is based on the work of S. Guerdoux, where more details can be found [5]. Section 3 details the efforts devoted to the computation of the mesh velocity, particularly for nodes of the material boundary. Finally, in Section 4, a comparison of the UL and ALE formulations is presented, on the examples of wire and square bar drawing processes.

2. ALE FORMALISM

A split ALE formulation is used and implemented in the FORGE3® software. Each time step is subdivided into three stages [6, 7]. First, a purely lagrangian computation provides the material velocity field ***v***. In the second stage, the mesh is regularised, which gives the mesh velocity field ***w***. After mesh updating, the variables are remapped from the old mesh to the new mesh (third stage).
The main difficulty of this approach is the mesh velocity computation [6].This is why this paper is focused on the second stage of the ALE method. Variable remapping is described elsewhere [5].
The second stage consists in relocating the nodes without changing the mesh topology. This r-adaptation aims at keeping the element shape regular, while maintaining or producing adequate mesh refinement in critical areas. The main difficulty is to accurately describe the evolution of the body surface [7]. The frontier of the mesh at $t+\Delta t$, noted $\delta M^{t+\Delta t}$, has to match the lagrangian updated frontier of the mesh M^t.

3. REZONING PHASE

3.1 General formulation

Rezoning aims at preserving a mesh of optimal quality. A weighted and iterative centering method is applied to compute the new node positions:

$$\mathbf{x}_m^{it} = \frac{1}{|\Gamma_m|} \sum_{e \in \Gamma_m} \mathbf{x}_{g_e}^{it-1} C_e^{it-1} \qquad (1)$$

where: Γ_m – the set of elements containing the node m, x_{ge} – the barycenter of element e, C_e^{it-1} - a weight factor, *it* – the iteration number considered. At boundary nodes, the barycenters of the facets containing the node m are considered, rather those of the elements.
The weight factor is introduced to provide an adaptive mesh with controlled element size and quality. It is a combination of two factors: a geometrical form factor to preserve the element quality and an adaptive factor to enforce a prescribed element size.

$$C_e^{it-1} = \alpha C_{f\,e}^{it-1} + (1-\alpha) C_{a\,e}^{it-1} \qquad (2)$$

$$C_{f\,e}^{it-1} = C_0 \frac{\left[V_e^{it-1}\right]^+}{\left(h_e^{it-1}\right)^3}$$

with

$$C_{a\,e}^{it-1} = \left(\frac{h_e^{it-1}}{h_e^{opt}} \right)^3 \qquad (3)$$

where: V_e - volume of element *e*, h_e- its average edge size, and α - a constant, between 0 and 1, depending on $C_{f\,e}^{it-1}$ [5]. The computation of the optimal size h_e^{opt} of the element *e* is based on the Zienkiewicz-Zhu (Z^2) error estimation [8, 9].
The mesh velocity w_m is derived from Equation (1):

$$w_m^{it} = \frac{(\mathbf{x}_m^0 - \mathbf{x}_m^{it})}{\Delta t} \qquad (4)$$

where: $\mathbf{x}_m^0$ - the coordinates of the initial node position, Δt – the time step.

3.2 Surface nodes : first procedure

At boundary nodes, a constraint has to be sastified by mesh velocity: the grid has to evolve along with the material boundaries of the domain. Hence, at each boundary node, the normal component of the mesh velocity is generally set equal to its material counterpart [4]:

$$\forall m \in \partial\Omega^{t}_{ALE} \qquad (v_m - w_m).n = 0 \qquad (5)$$

where: v_m – material velocity at node m, n - either a consistent normal to the free surface of the workpiece, or the outward contact normal.
Using this condition (5) to compute a drawing process with a dominant tangential material flow has been unsuccessful (figure 1). The free surface wrinkles, as the edges were not preserved, generating numerical mesh distortion.

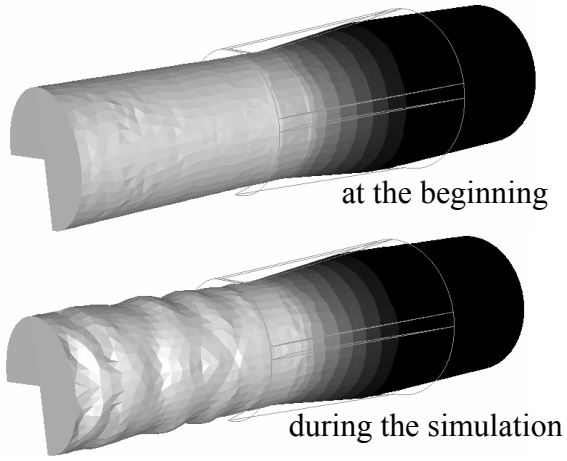

Figure 1. Test of the formulation using equation (5) for surface node movement, in round wire drawing: major surface oscillations are observed.

Waviness first appeared at the entry and exit lines of the deformation zone. For a node located on one of these lines, the upstream facets are parallel to the drawing axis, whereas the downstream facets are parallel to the die cone: the consistent normal is therefore slightly oriented in the axial direction. Following equation (5) above, the high tangential material velocity leads to a rather large tangential mesh velocity. The node moves significantly in the material flow direction, contrary to expectations. When modelling stationary processes with an ALE method, the mesh displacement in the material flow direction should be small or even null, whereas it is free in the other directions in order to respect the deformation of the surfaces.

3.3 Surface nodes : second procedure

A new procedure, namely a projection technique, is implemented to tackle boundary preservation. In a first step, the lagrangian update of the surface at time t+Δt is locally computed (Figure 2). Then, the nodes positioned by the rezoning algorithm (see section 3.1), are projected onto this updated surface.
A boundary node m can be located at a corner, on an edge or on a plane or curved surface. The status of m is determined by a simple local modal analysis of the normal vectors of the facets containing this node, performed at each time step [5]. Different projection strategies are applied according to these three categories.

Plane or curved surfaces

The updated lagrangian surface is built locally. Only the first neighbours of the studied node m are considered (patch P^{t}_{mALE}, Figure 2).

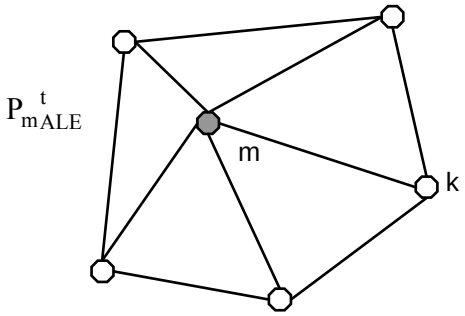

Figure 2. Patch P^{t}_{mALE} of the faces of the ALE mesh containing node m.

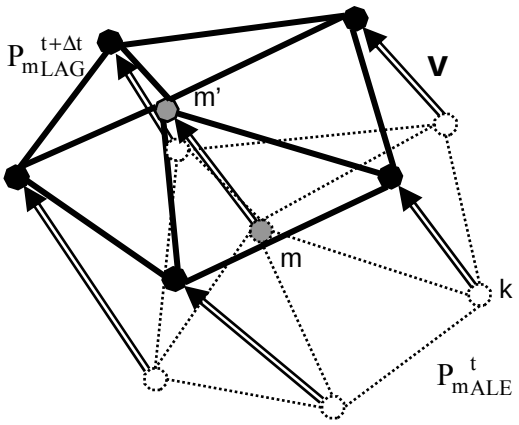

Figure 3. Lagrangian updating of the patch P^{t}_{mALE}.

The updated lagrangian positions of node m and its neighbours are computed using the material velocity (Figure 3):

$$\forall k \in P_{m\,ALE}^{\ t} \quad x_{k,LAG}^{t+\Delta t} = x_{k,ALE}^{t} + v_k^t \, \Delta t \quad (6)$$

where: $x_{k,LAG}^{t+\Delta t}$ - lagrangian update of the first neighbour k of node m, $x_{k,ALE}^{t}$ - its non-updated coordinates, v_k^t - material velocity of k at t.
They form the virtual lagrangian update $P_{mLAG}^{t+\Delta t}$ of P_{mALE}^{t}.
The barycentered position of node m is projected onto the patch $P_{mLAG}^{t+\Delta t}$ as the new position of node m on the ALE mesh (Figure 4).

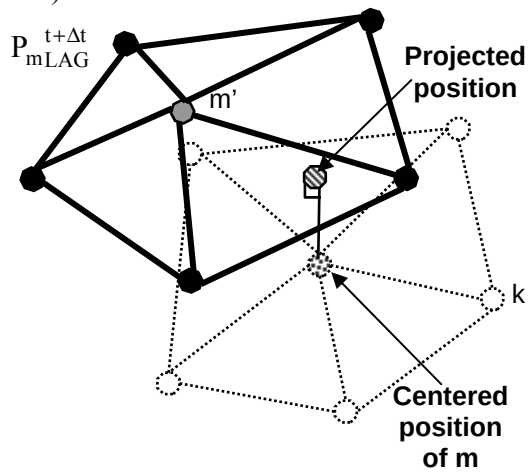

Figure 4. Projection of the centered position of m onto the patch $P_{mLAG}^{t+\Delta t}$.

The mesh velocity is deducted from the position of the projected node:

$$w_m^{it} = \frac{(\mathbf{x}_m^0 - \mathbf{x}_P^{it})}{\Delta t} \quad (7)$$

where: x_p^{it} - the coordinates of the node projection.

Edges
A node on an edge must stay on the edge after rezoning. Hence, it is projected onto the lagrangian update of the edge. This edge is locally described by node m and its upstream and downstream neighbours along the edge (Figure 5). After computing their lagrangian positions, noted k'_i, two segments [m' k'_i] are obtained. The centered position (provided by (1)) is projected on each segment. The closest projected point (Figure 6) is used to determine the new mesh velocity at node m according to Equation (7).

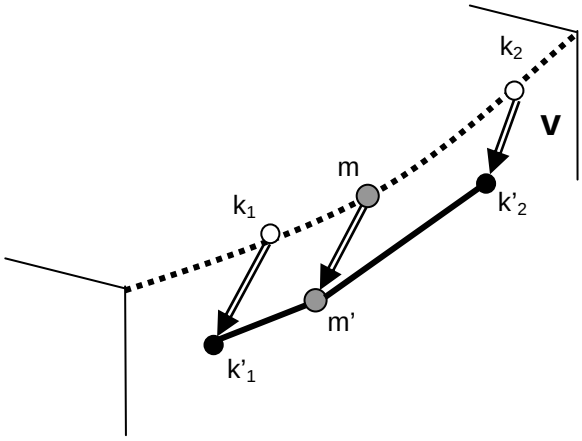

Figure 5. Local virtual lagrangian updating of a node m located on the edge.

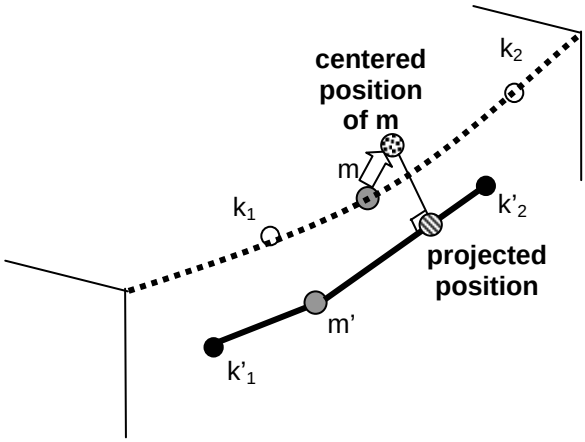

Figure 6. Projection of the centered position of node m on segments [m' k'_i].

Corner
For corner nodes, the mesh velocity is set equal to the material velocity.

Specific boundary planes
When modelling the steady state of a continuous process, a fixed area in space must be defined. This area is limited in the main flow direction by upstream and downstream extreme cross-sections, here called specific boundary planes. Nodes belonging

to these planes are not allowed to move outside the defined space. They are eulerian, with a null mesh velocity. Nodes located at the edges and corners of the boundary planes are not exactly projected as described above. In fact, material keeps flowing outside these arbitrary planes, so that these mesh corners are not true material corners. Therefore, the corner node belonging to such a boundary plane is projected like an edge node. Similarly, nodes on an edge of the boundary plane are handled like nodes located on a surface.

3.4 Sub-stepping

The projection procedure is applied locally, on the patch made of the first neighbours. If the computational time step is too large, the projected node may be outside this patch. To overcome this limitation, the time step is divided into several smaller sub-steps during rezoning. The size of the sub-step Δt_{ALE} is limited by the mimimum edge length of a mesh element l_{min}:

$$\Delta t_{ALE} = \frac{l_{min}}{v_{max}} \tag{8}$$

where: v_{max} – maximum material velocity
During these reduced time steps, the material velocity is regarded as constant. Therefore, it has to be transported during the various sub-steps. A simple inverse interpolation from one mesh to the other is locally used.

4. TESTS AND RESULTS

The new formulation is compared to a more standard Lagrangian formulation [1].

4.1 Model definition

Comparisons have been carried out for two 3D drawing processes: wire drawing and rectangular sectional drawing. In the first process, the wire of initial diameter 10 mm is drawn through a conical die of semi-angle 7°, down to 8 mm diameter. In the second process, a 10-mm round bar is drawn into a rectangular section 6 x 8 mm². In both cases, the reduction in area is around 35%.
Other process conditions are identical in the two processes. An aluminium alloy, AA5083, is modelled as elastic-viscoplastic (Table 1) with thermo-mechanical coupling.

Table 1: Material properties.

consistency	445 Mpa
strain rate sensitivity index	0.016
strain-hardening index	0.168
young modulus	73 GPa
ν	0.3

Friction follows Coulomb's law (μ= 0,02). The dies are rigid and isothermal, described by a surface mesh only. The drawing velocity is 100 mm/s, prescribed at the nodes of the front side of the workpiece. Only one quarter of the process is modelled due to symmetry. The unstructured workpiece mesh is composed of tetrahedral mini-elements [1].
When modelling with the ALE formulation, the steady state of the geometry is directly represented, with the conical transition between the preformed and the drawn wire (Figure 7a). On the contrary, UL starts from a cylindrical billet (Figure 7b) and is forced to model the transient stage until reaching the steady state.
In ALE, the two boundary planes defined above are treated somewhat differently. At the rear side, the nodes are eulerian, i.e. no movement is allowed. At the front side, they are only fixed in the direction of the material flow. ALE simulations were carried out with or without adaptivity.

4.2 Results

During the ALE computation with the second formulation (paragraph 3.3), the domain geometry is well preserved. No surface oscillations appear (Figure 7d), contrary to Figure 1 under the same conditions.

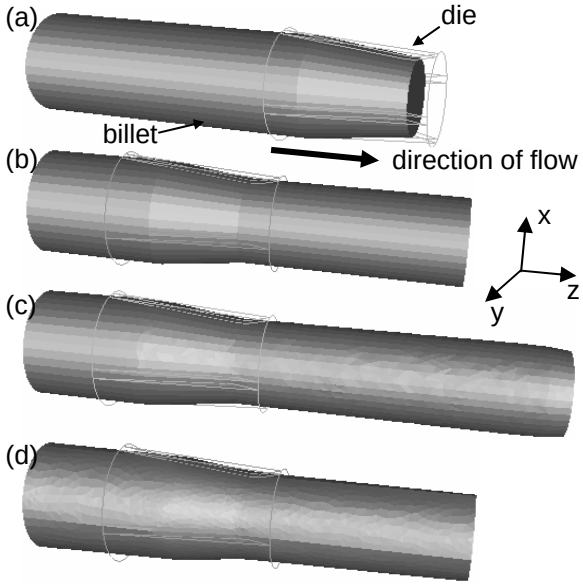

Figure 7. Wire drawing model at the beginning (a,b) and end (c,d) of the UL simulation (a,c) and the ALE simulation (b,d).

With the rectangular section, the same surface mesh quality is obtained (Figure 8b).

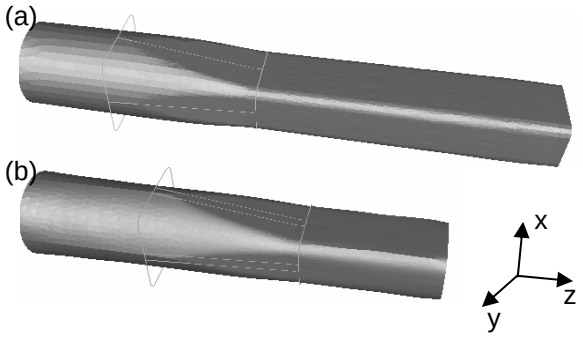

Figure 8. Rectangular section drawing model (x = 6 mm, y = 8 mm) at the end of (a) the UL simulation and (b) the ALE simulation.

As can be observed in the cross-sections of Figures 9 and 10, elements keep a better equiaxed shape with the ALE formulation, compared to UL. In the UL simulation and in the ALE simulation without adaptivity, the element size was equal to 0.75 mm. In the ALE simulation with adaptivity, a finer mesh was located in the critical deformation zone: element size of about 0.5 mm for wire drawing and element size of about 0.3 mm for rectangular section drawing. Furthermore, the other regions in the wire drawing model were meshed with bigger elements (element size of 1 mm).

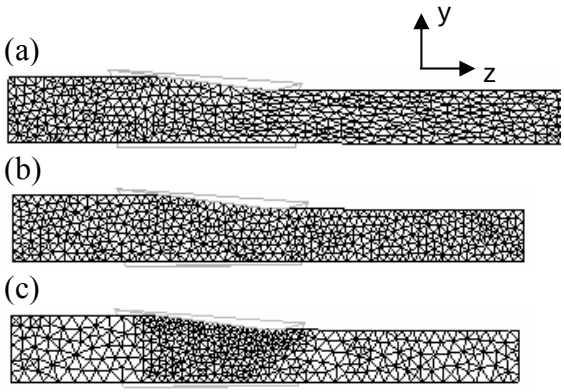

Figure 9. Mesh for the wire drawing at the end of (a) the UL simulation, (b) the ALE simulation without adaptivity and (c) with adaptivity.

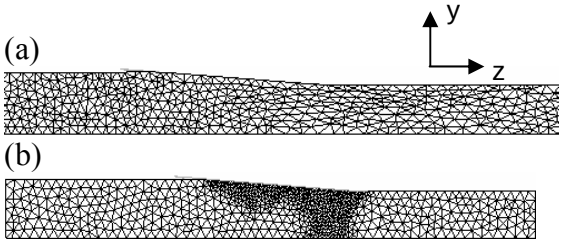

Figure 10. Mesh for the rectangular section drawing at the end of (a) the lagrangian simulation, (b) the ALE simulation with adaptivity.

The adaptive ALE computation has a locally finer mesh, which could have resulted in a smaller time-step compared to UL. Sub-stepping during node rezoning, as explained in paragraph 3.4, allowed the same time-step to be used in all simulations: $5*10^{-3}$ s for wire drawing and 10^{-3} s for rectangular section drawing.
The UL simulation is carried out without remeshing. The computational time of the UL simulation and the computational time of the ALE simulation without adaptivity are similar for wire drawing. ALE simulations with adaptivity require larger computational times because of higher numbers of elements in the deformation zone.

Figures 11 and 12 show the distributions of drawing stresses at the end of simulations (corresponding to the steady-state). Very few differences can be noticed between the distributions provided by ALE simulations and those provided by UL simulations. Regarding wire drawing, a more compressive drawing stress is computed with the adap-

tive ALE formulation in two regions: in the contact zone and at the drawn wire centre (Figure 11). At the entry zone of the rectangular section drawing, the adaptive ALE computation gives a larger zone with high compressive drawing stresses (Figure 12).

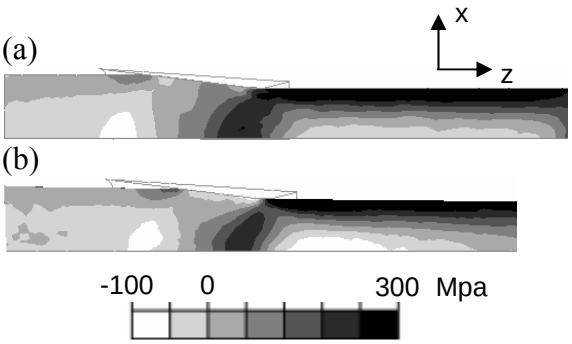

Figure 11. Wire drawing process: distribution of drawing stress at the end of (a) the UL simulation and (b) the ALE simulation with adaptivity.

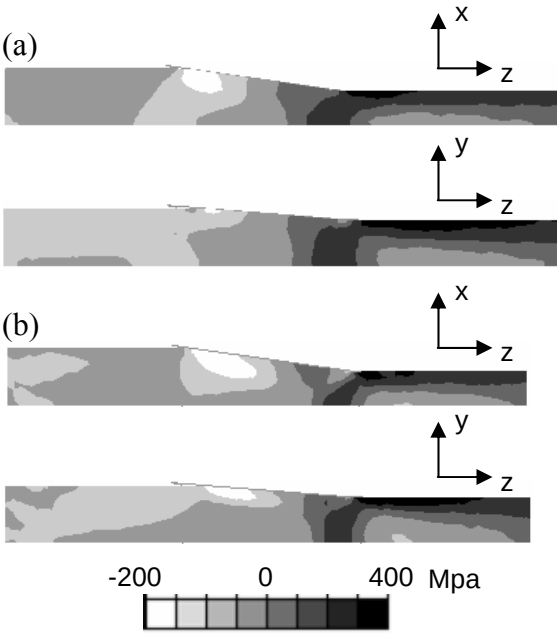

Figure 12. Rectangular section drawing process: distribution of drawing stresses at the end of (a) the UL simulation and (b) the ALE simulation.

As can be observed in Figure 13, the distribution of strain rates is more precise with the adaptive ALE computation.

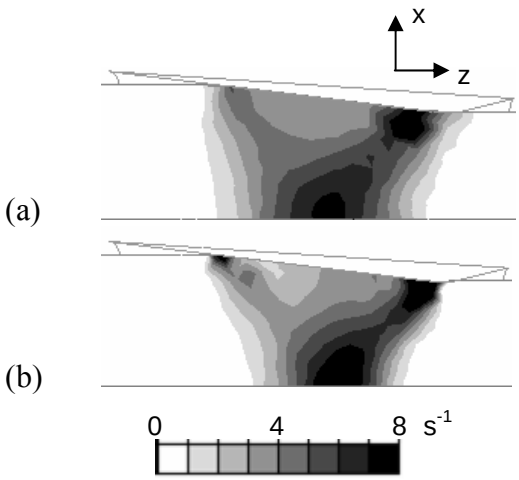

Figure 13. Wire drawing process: equivalent strain rate map at the end of (a) the UL simulation and (b) the ALE simulation.

Compared to the UL formulation, the adaptive ALE formulation allows to automatically getting finer elements in the critical deformation zone, leading to results of higher accuracy. Using an adaptive node rezoning, the mesh refinement is kept in this zone.

5. CONCLUSION

The proposed ALE formulation has been applied successfully to two drawing processes. The mesh is unstructured and composed of tetrahedral elements. In this case, it is found that stationary processes with large tangential velocity require a more consistant rezoning method to respect material boundaries.

Boundary nodes are projected onto the updated Lagrangian surface. Complex domain geometries, such as the rectangular rod with edges and corners, are well described. Furthermore, good element shapes and initial refinements can be preserved during the entire simulation.

The ALE method, coupled with adaptivity, automatically performs refinements in critical areas. It provides results of better quality than those obtained with the UL formulation. In spite of the finer mesh, increment time does not need to be reduced, thanks to the use of sub-stepping during rezoning.

However, the computational times of ALE simulations with adaptivity are high. Considering an identical accuracy of results for the UL simulation, it can be expected that the adaptive ALE formulation provides better computational times.

References

1. Chenot J.L., Fourment L., Coupez T., Ducloux R., Wey E., “Forge3® : a general tool for practical optimisation of forging sequence of complex 3-D parts in industry”, Proc. ICFT’98, eds, Institution of Mechanical Engineers, Birmingham, 1998, pp 113-122.
2. Coupez T., Chenot J.L., “Mesh topology for mesh generation problems - Application to three-dimensional remeshing”, Proc. NUMIFORM 92, eds, Chenot J.L et al, Balkema A.A., Rotterdam, 1992, pp. 237-242.
3. Dvorkin E. N., Petöcz E.G., “An effective technique for modelling 2D metal forming processes using an Eulerian technique”, Engineering Computations, vol. 10, 1993, pp. 323-336.
4. Gadala M.S., “Recent trends in ALE formulation and its applications in solid mechanics”, Computer Methods in Applied Mechanics and Engineering, 2004, vol. 193, pp. 4247-4275.
5. S. Guerdoux, “Numerical simulation of the friction stir welding process”, PhD Thesis, Mines Paris - Paristech, Sophia-Antipolis, 2007.
6. Boman R., Papeleux L., Bui Q.V., Ponthot J.P., “Application of the Arbitrary Lagrangian Eulerian formulation to the numerical simulation of cold roll forming process”, Journal of Materials Processing Technology, vol. 177, 2006, pp.621-625.
7. Aymone J.L.F, Bittencourt E., Creus G.J., “Simulation of 3D metal-forming using an arbitrary Lagrangian-Eulerian finite element method”, Journal of Materials Processing Technology, vol. 110, 2001, pp. 218-232.
8. Wisselink H.H., Huétink J., “3D FEM simulation of stationary metal forming processes with applications to slitting and rolling”, Journal of Materials Processing Technology, vol. 148, 2004, pp. 328-341.
9. Zienkiewicz O.C., Zhu J.Z., "A simple error estimator and adaptive procedure for practical engineering analysis", International Journal for Numerical Methods in Engineering, vol. 24, 1987, p. 337-357.
10. Boussetta R., Coupez T., Fourment L., “Adaptive remeshing based on a posteriori error estimation for forging simulation”, Computer Methods in Applied Mechanics and Engineering, vol. 195, 2006, pp. 6626-6645.